Relating radar-sounding measurements of ice fabric to ice-flow enhancement of Rutford Ice Stream

Tom Jordan [1,2], Alex Brisbourne[3], Carlos Martin [3], Rebecca Schlegel [4], Dustin Schroeder [2,5], Andrew Smith[3]

1. School of Geographical Sciences, University of Bristol, Bristol, UK.
2. Department of Geophysics, Stanford University, Stanford, USA.
3. British Antarctic Survey, Cambridge, UK.
4. Department of Geography, Swansea University, Swansea, UK.
5. Department of Electrical Engineering, Stanford University, Stanford, USA.

Contact: tom.jordan@bris.ac.uk

Ice fabric: what is it and what properties can we measure with radar?

Ice fabric = orientation distribution of ice crystals.

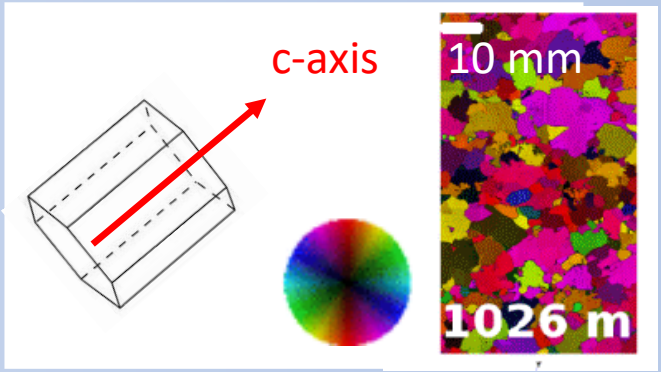

With polarimetric radar-sounding we measure the strength and orientation of a `vertical girdle' fabric: **horizontal anisotropy**

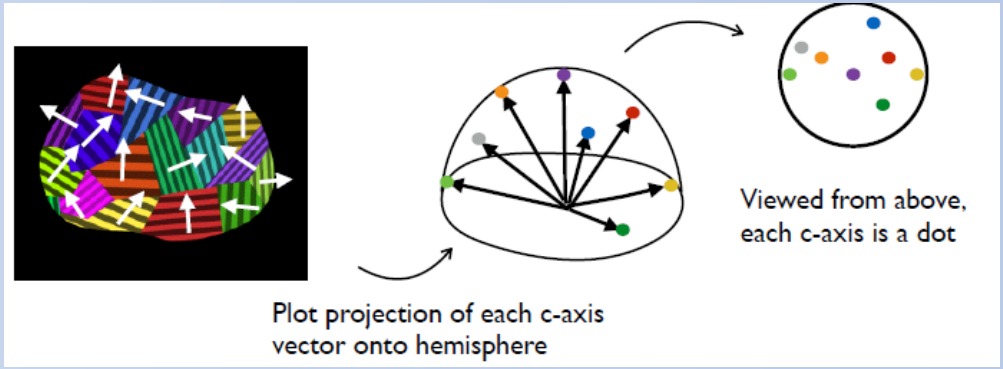

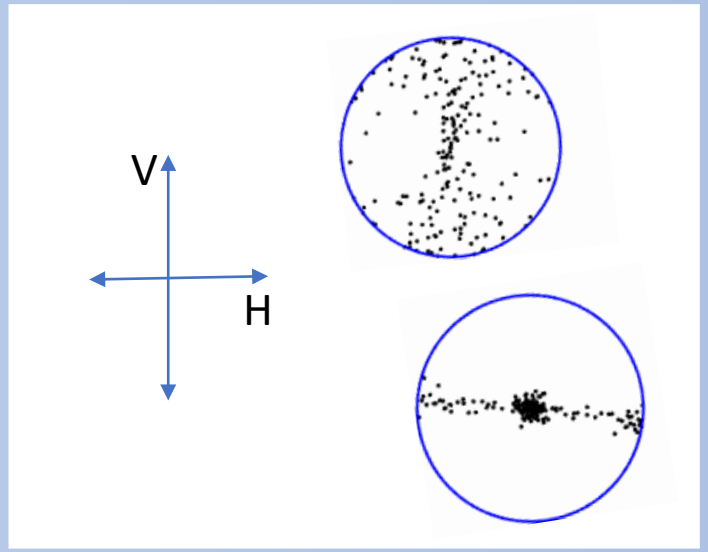

NEEM fabric (upper) from Montagnat et al. 2014 TC, Schmid image (lower) from Ian Hewitt, Karthaus notes

Key question: how do girdle fabrics influence near-surface deformation of Rutford Ice stream?

Ice fabric results in anisotropic ice rheology: `harder or softer to strain in different directions'

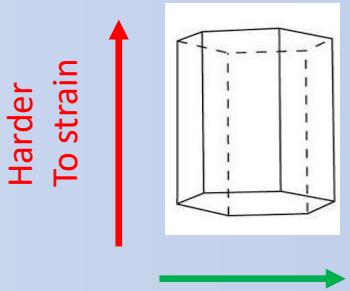

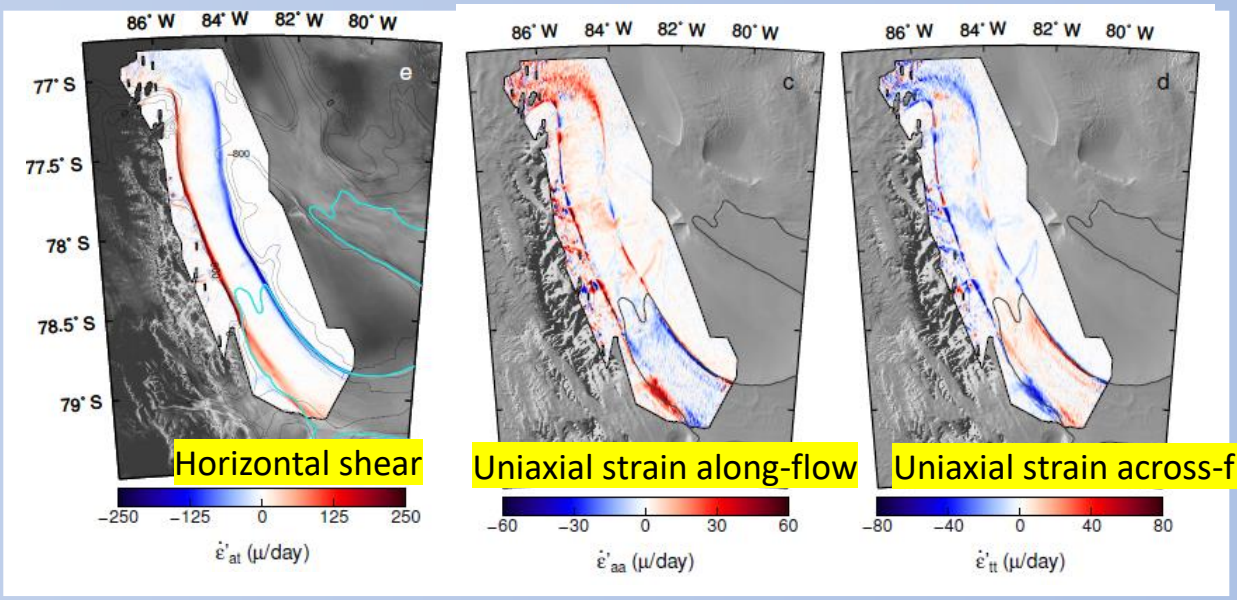

Rutford Ice Stream surface strain rates (Minchew et al. 2017, JGR)

Complex ice-surface deformation signature:

- Transition from shear-dominance at margins to greater influence of uniaxial-strain at ice-stream center.
- Extension and compression can both act along- & across- flow.

Preview of presentation: methodology

1. Polarimetric radar-sounding measurements (ApRES) & coherence analysis

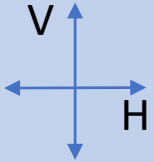

ApRES Image from Nichols et al. 2015, J. Glac.

2. Modeling radar constraints on anisotropic ice rheology

$$\begin{pmatrix} D_{11} \\ D_{22} \\ D_{33} \\ D_{12} \\ D_{13} \\ D_{23} \end{pmatrix} = \psi_0 \begin{pmatrix} \psi_{1111} & \psi_{1122} & \psi_{1133} & 0 & 0 & 0 \\ \psi_{1122} & \psi_{2222} & \psi_{2233} & 0 & 0 & 0 \\ \psi_{1133} & \psi_{2233} & \psi_{3333} & 0 & 0 & 0 \\ 0 & 0 & 0 & \psi_{1212} & 0 & 0 \\ 0 & 0 & 0 & 0 & \psi_{1313} & 0 \\ 0 & 0 & 0 & 0 & 0 & \psi_{2323} \end{pmatrix} \begin{pmatrix} S_{11} \\ S_{22} \\ S_{33} \\ S_{12} \\ S_{13} \\ S_{23} \end{pmatrix}$$

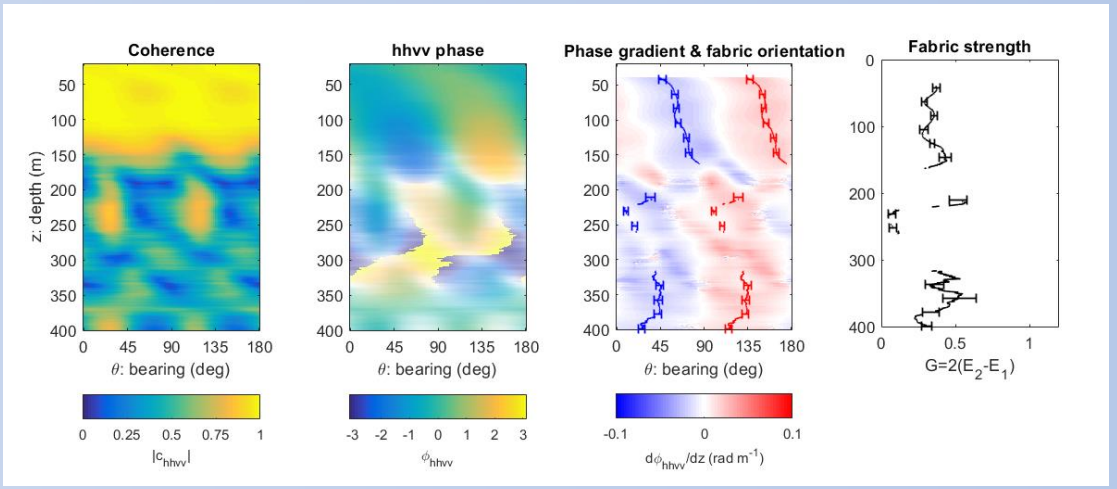

Unconstrained

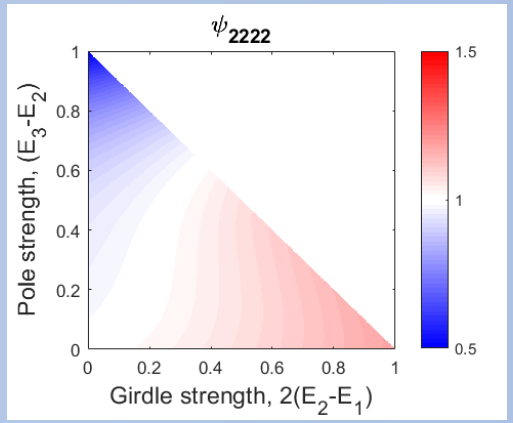

Measured by radar

Preview of presentation: results

3. Spatial variability in fabric within Rutford

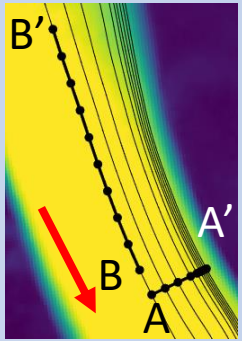

Ice flow direction

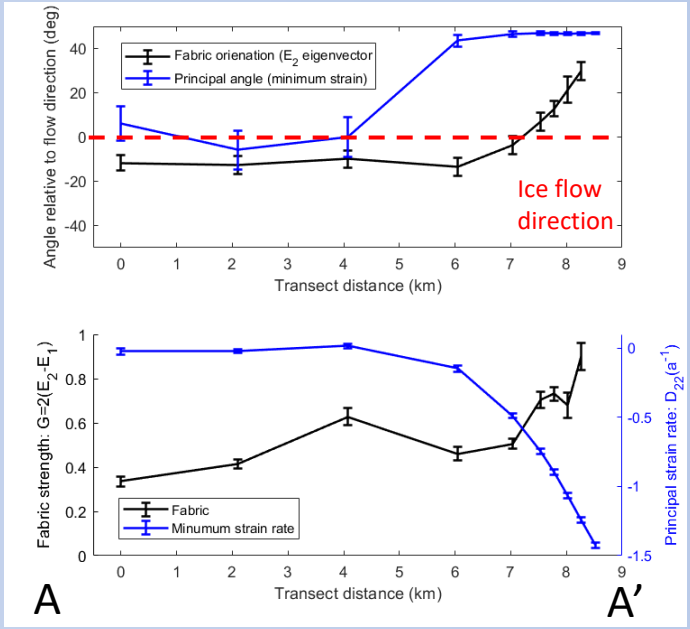

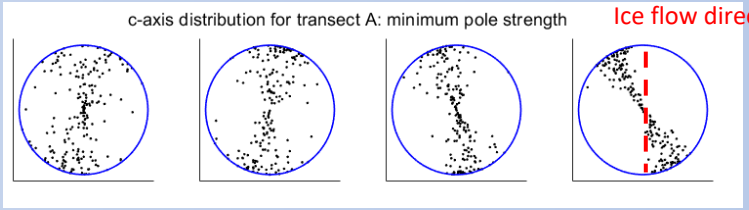

4. Radar bounds on anisotropic ice rheology

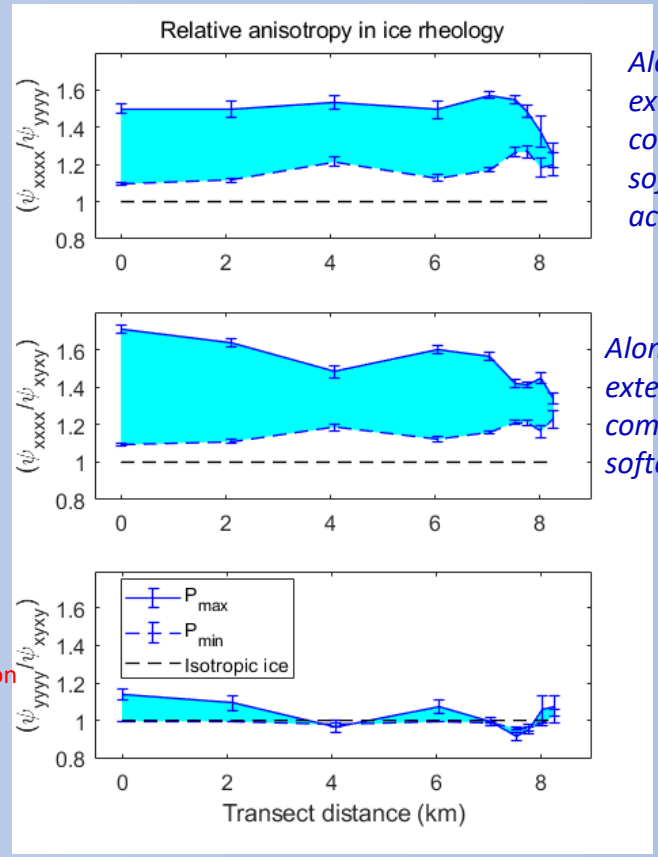

Along-flow extension/ compression softer than across-flow

Along-flow extension/ compression softer than shear

Contents

1.1 Glaciological setting and measurement sites

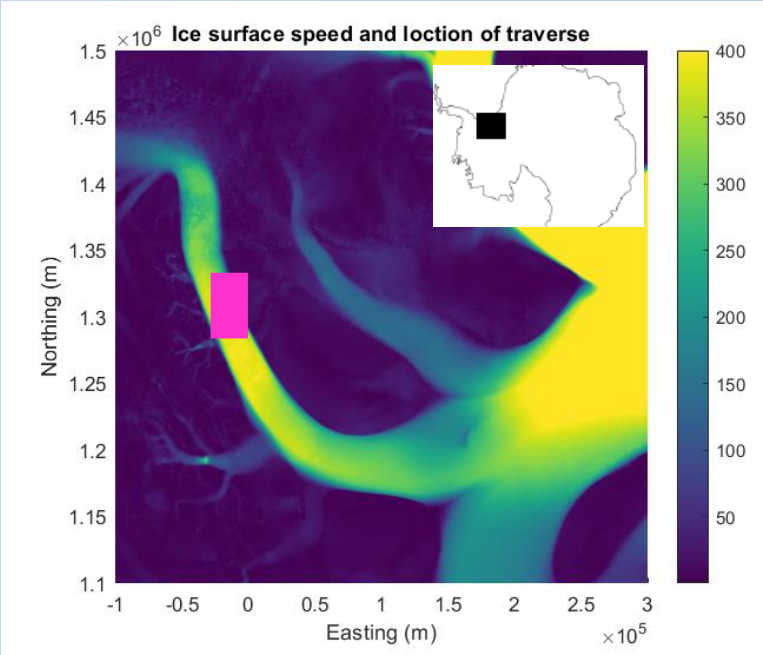

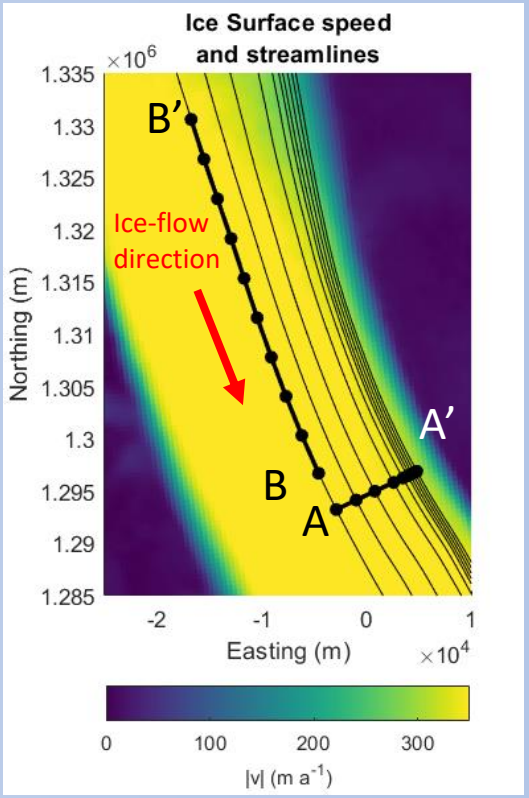

Data consists of two transects of 10 measurement sites in Rutford Ice Stream, West Antarctica. Collected as part of the NERC BEAMISH project.

Transect A: tangential to ice-flow, begins at central stream- and heads towards shear margin

Transect B: parallel to ice-flow along central streamline

Quad-polarimetric acquisitions using an ApRES (Autonomous-phase sensitive radio echo sounder).

1.2 Polarimetric data analysis

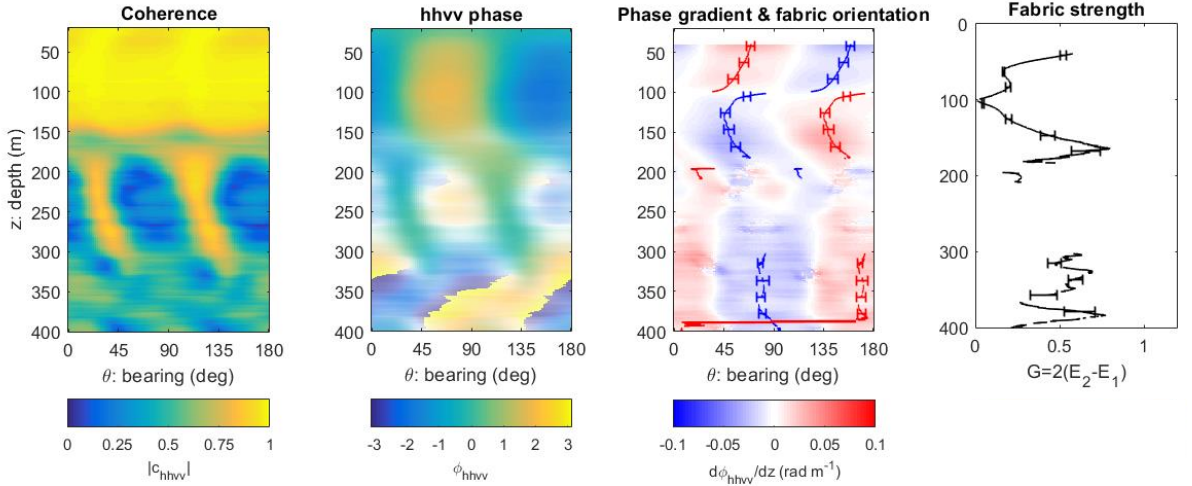

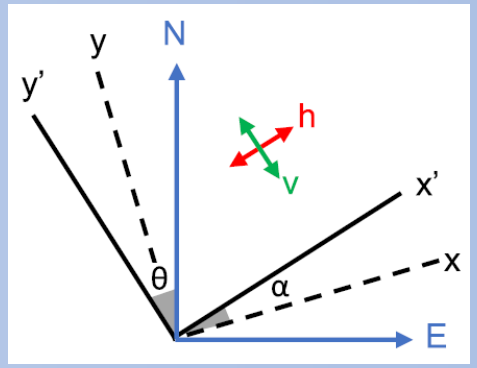

$$c_{\mathrm{hhvv}} = \frac{\sum_{i=1}^{N} s_{hh,i} \cdot s_{vv,i}^{*}}{\sqrt{\sum_{i=1}^{N} |s_{hh,i}|^2} \sqrt{\sum_{i=1}^{N} |s_{vv,i}|^2}}$$

$$\phi_{\mathrm{hhvv}} = \arg(c_{\mathrm{hhvv}})$$

$$\left| \frac{d\phi_{\mathrm{hhvv}}(\alpha = 0°, 90°)}{dz} \right| = \frac{d\delta}{dz} = \frac{4\pi f}{c} \frac{\Delta\epsilon'(E_2(z) - E_1(z))}{2\sqrt{\epsilon}}$$

Based upon polarimetric coherence methodology (Dall 2009 & Jordan et al. 2019) where depth-azimuth properties of hhvv coherence phase & vertical gradient are used to extract girdle properties

Refinements to previous methodology: basis transform from quad-polarized to `multi-polarization plane' data, incorporation of antenna alignment uncertainty, improved automation.

1.3 Polarimetric backscatter model

hhvv phase & gradient for depth-invariant orientation (anisotropic scattering)

hhvv phase & gradient for 90 deg azimuthal rotations (isotropic scattering)

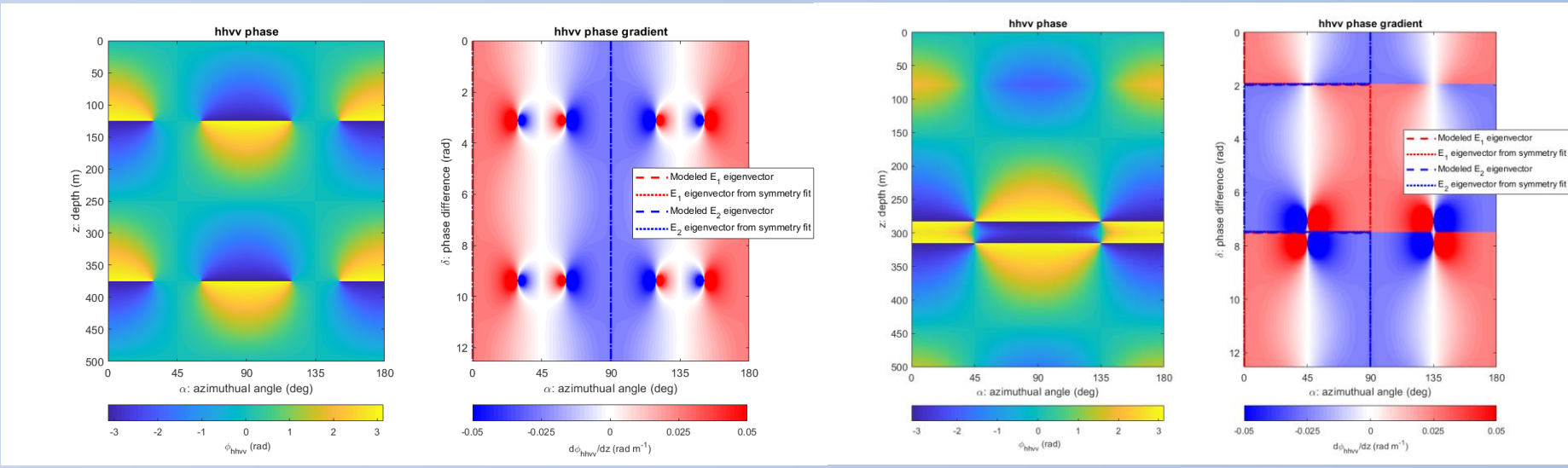

Forward model of hhvv phase for radio propagation & backscatter in a birefringent ice-sheet (Fujita et al. 2006, Jordan et al. 2019) used to constrain polarimetric data analysis.

Model indicates that fabric eigenvectors can be determined from azimuthal angle that maximize 180-degree azimuthal reflection symmetry of hhvv phase. This property holds exactly for depth-invariant fabric or 90 degree rotations in the ice column (Disclaimer: non 90-degree rotations result in reflection-symmetry breaking & fit biases).

1.4 Polarimetric data analysis: Transect A

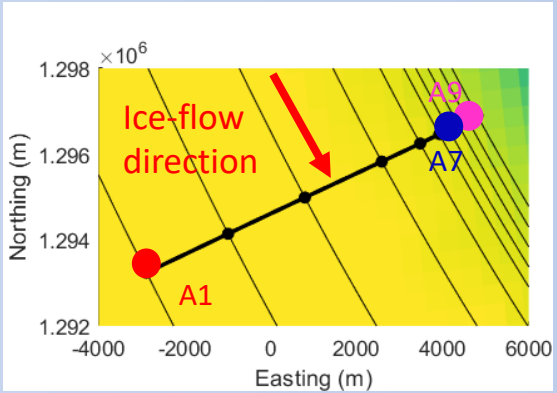

When interpreting spatial patterns focus on high coherence band in the near-surface: 40 < z< 90 m (indicated by green box in top plot).

Blue & red lines indicate E1 and E2 eigenvectors as a function of ice depth. Filter out poorer fits and low coherence regions.

Transparency of phase and phase gradient plots indicates coherence strength..

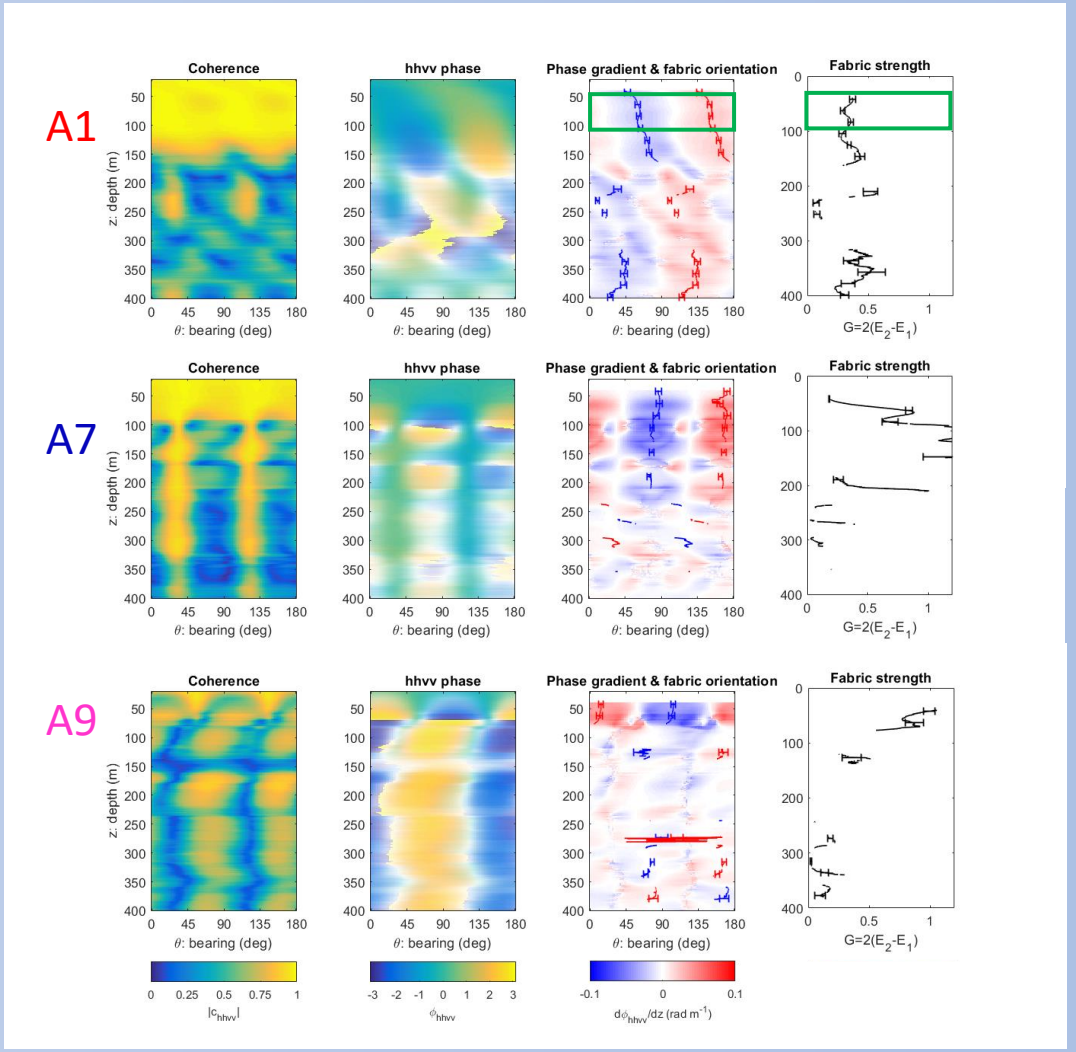

1.5 Polarimetric data analysis: Transect B

Upstream sites (B8-B10) indicate rapid depth-transition in fabric orientation (~90 degrees) at z~ 100m Focus on two `depth units' when comparing sites (green and black boxes in bottom plot).

Downstream sites (B1-B7) have no depth-transition.

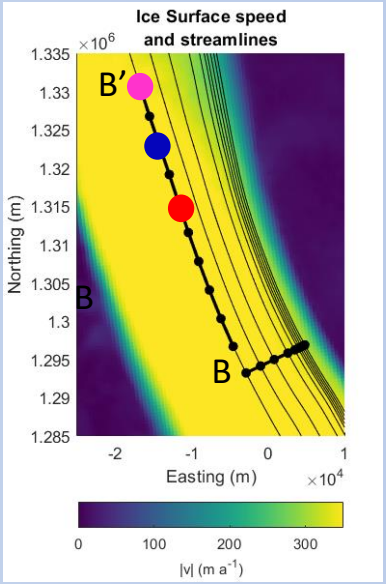

B6

B8

B10

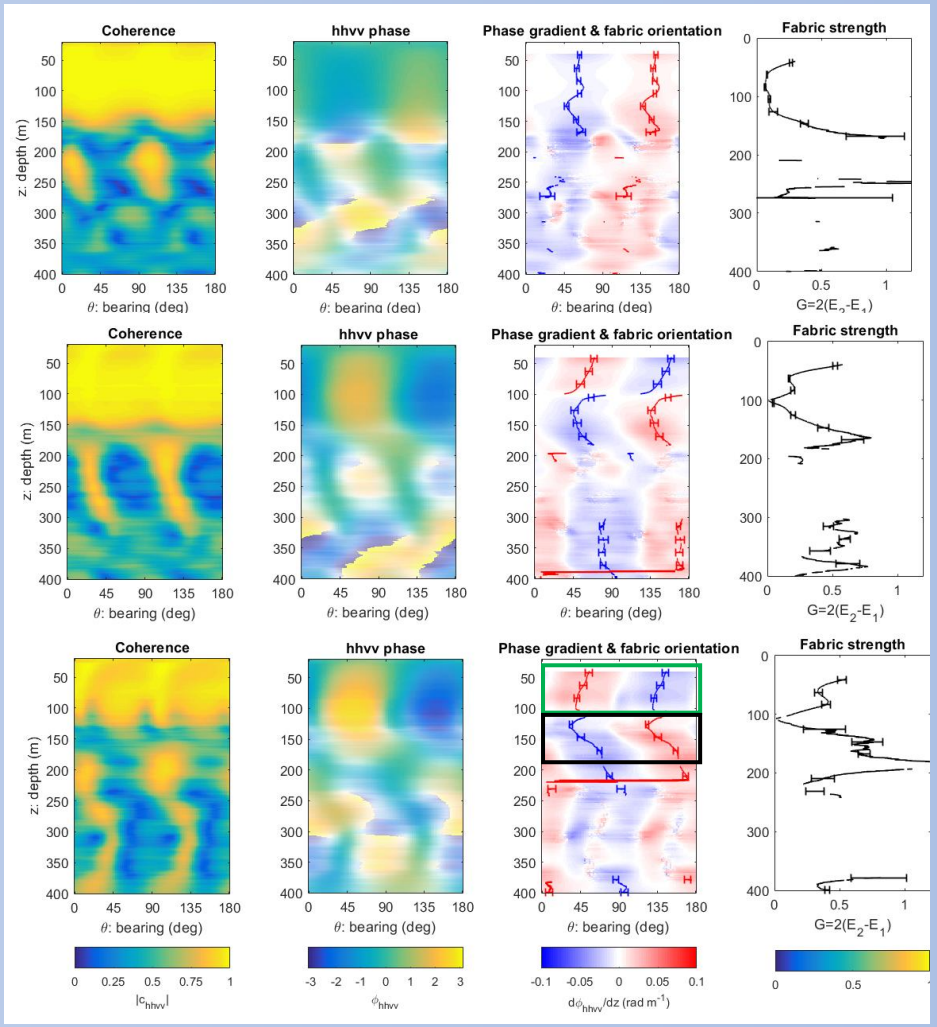

2.1 Girdle-pole decomposition of fabric eigenvalue space

P is unconstrained

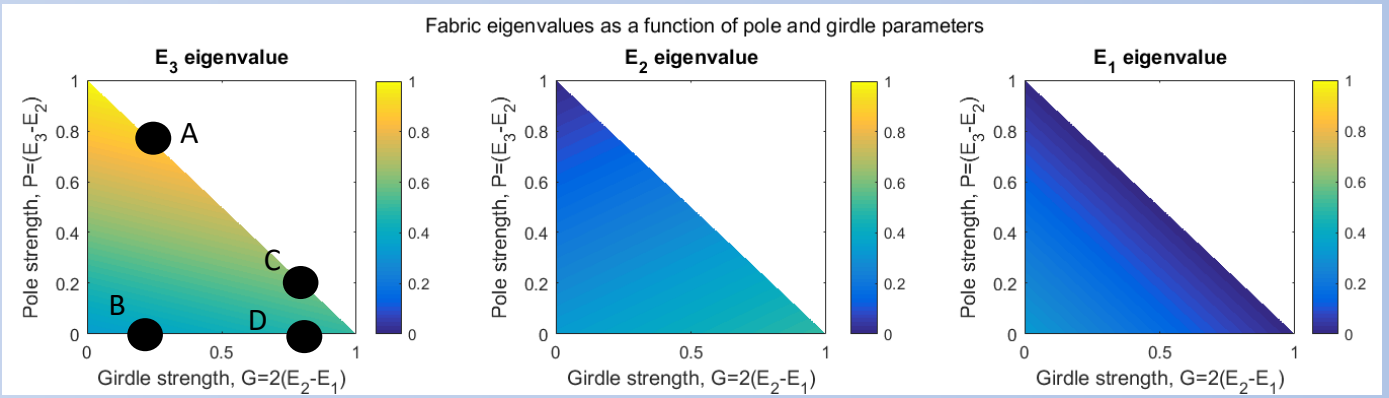

G is measured by radar

Prior step to rheological modelling is to define fabric parameter-space in terms of what we can/cannot measure.

Assume fabric eigenvalue convection E3>E2>E1 with E3 vertical. E3+E2+E1=1, means we reduce to 2 DOF: pole (P) & girdle strength (G) defined on [0,1]

A

Upper bound on P for G=0.2 (E1=0, E2=0.1, E3=0.9)

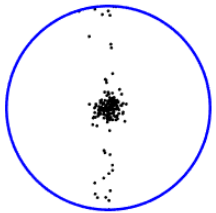

B

Lower bound on P for G=0.2 (E1=0.267, E2=E3=0.367)

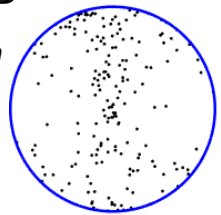

C

Upper bound on P for G=0.8 (E1=0, E2=0.4,E3=0.6)

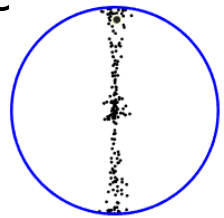

D

Lower bound on P for G=0.8 (E1=0.067, E2=E3=0.467)

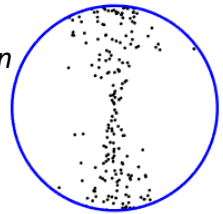

The pole strength (and set of three eigenvalues) is better constrained for greater girdle strengths

2.2 Rheological modelling: effect of girdle strengthening

$$\begin{pmatrix} D_{11} \\ D_{22} \\ D_{33} \\ D_{12} \\ D_{13} \\ D_{23} \end{pmatrix} = \psi_0 \begin{pmatrix} \psi_{1111} & \psi_{1122} & \psi_{1133} & 0 & 0 & 0 \\ \psi_{1122} & \psi_{2222} & \psi_{2233} & 0 & 0 & 0 \\ \psi_{1133} & \psi_{2233} & \psi_{3333} & 0 & 0 & 0 \\ 0 & 0 & 0 & \psi_{1212} & 0 & 0 \\ 0 & 0 & 0 & 0 & \psi_{1313} & 0 \\ 0 & 0 & 0 & 0 & 0 & \psi_{2323} \end{pmatrix} \begin{pmatrix} S_{11} \\ S_{22} \\ S_{33} \\ S_{12} \\ S_{13} \\ S_{23} \end{pmatrix}$$

Anisotropic flow law for linear orthotropic rheology D: strain rate, ψ: fluidity (viscosity inverse) , S: deviatoric stress (Gillet Chaulet et al. 2005, J Glac., Martin et al. 2009, JGR)

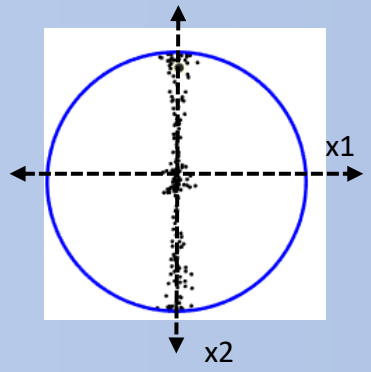

Girdle strengthening results in `anisotropy of uniaxial deformation' (ψ1111 decreases and ψ2222 increases with G).

Cannot constrain shear with radar as contours are ~ horizontal (i.e. shear is function of pole strength).

Horizontal fluidity components: principal coordinates (x1,x2)

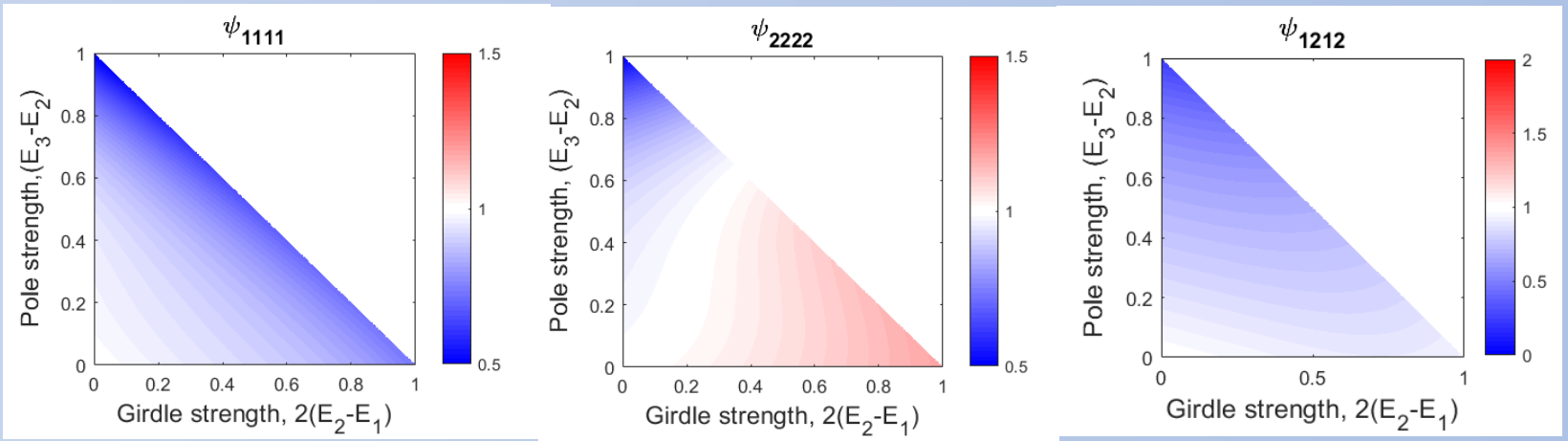

2.3 Rheological modelling: effect of girdle rotation

Consider rotational transform of fluidity tensor from principal (x1,x2) to ice-stream coordinate system (x,y)

Convention: when θ_{flow}=0 degs x2 (girdle plane) is aligned with x (flow).

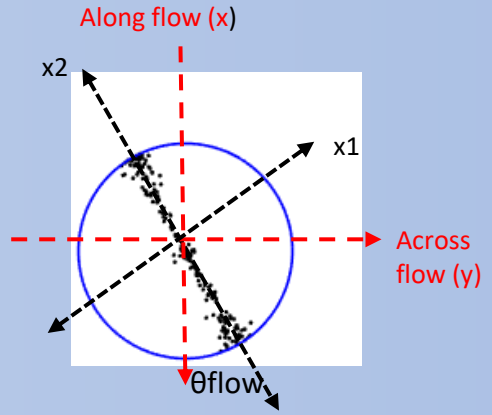

Uniaxial horizontal fluidity components: ice-stream coordinates (x,y)

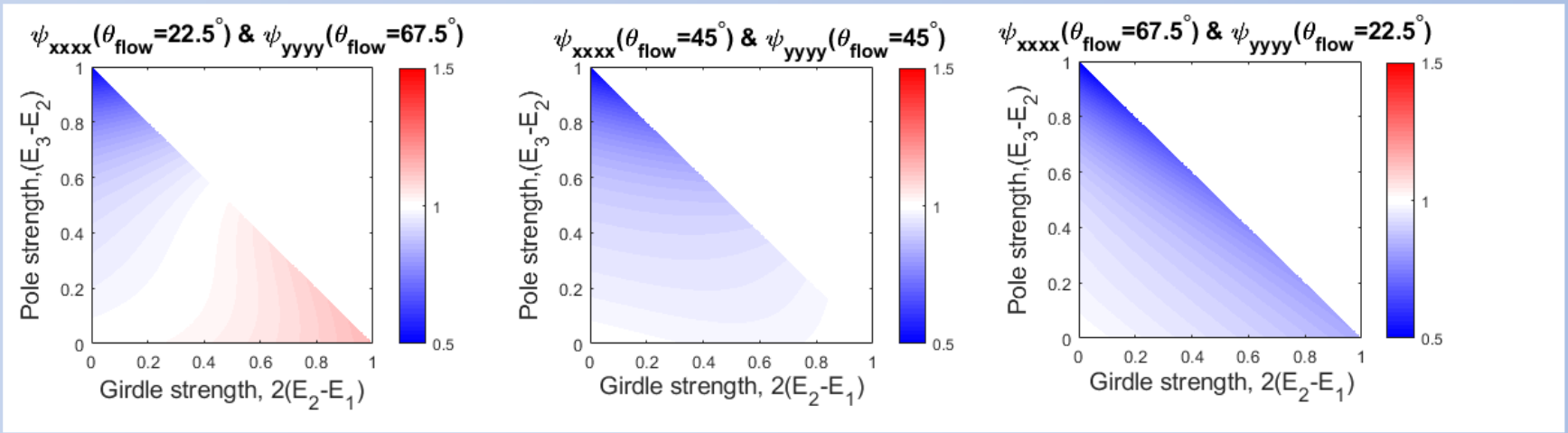

Girdle rotation results in `hard' (x1) and `soft' (x2) uniaxial strain directions changing with respect to ice-stream coordinates (x,y). Note: rotation transform has negligible effect on shear.

3.1 Spatial variation in ice fabric: Transect A

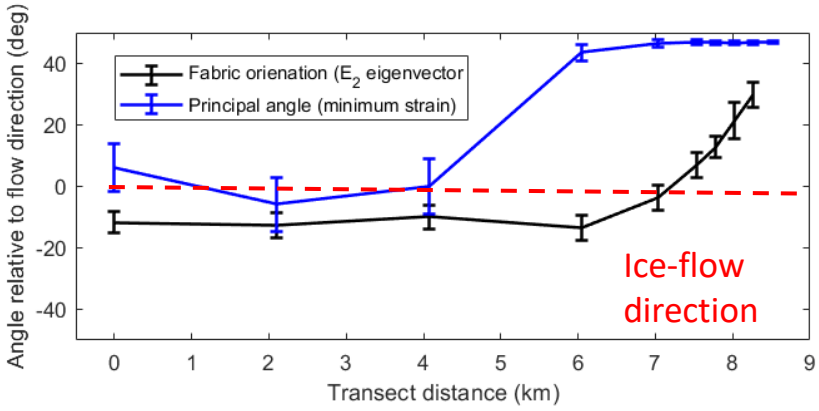

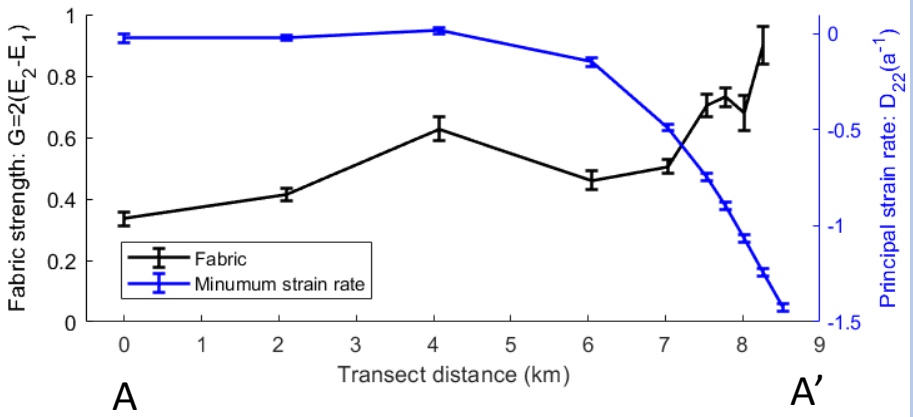

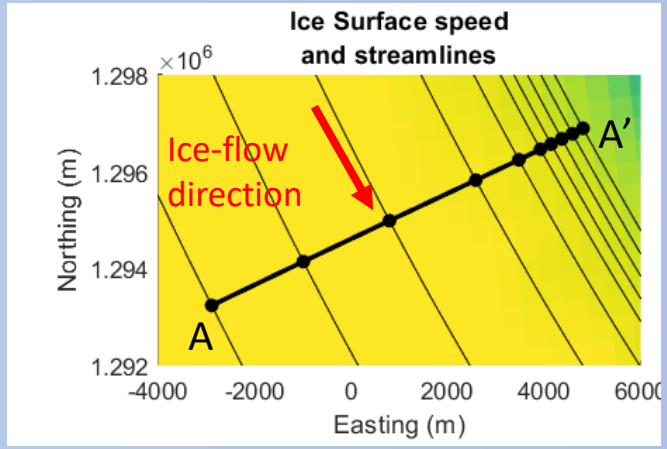

Overall tendency for girdle-alignment with compression axis. (When theta=0 degs, fabric and compression axis are aligned with flow)

Girdle strength increases with compression magnitude

*Fabric results are depth-averaged on 40 < z < 100 m.

3.2 Synthetic c-axis distributions: Transect A

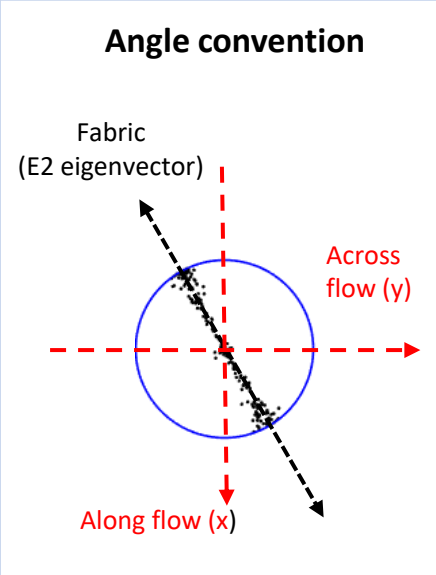

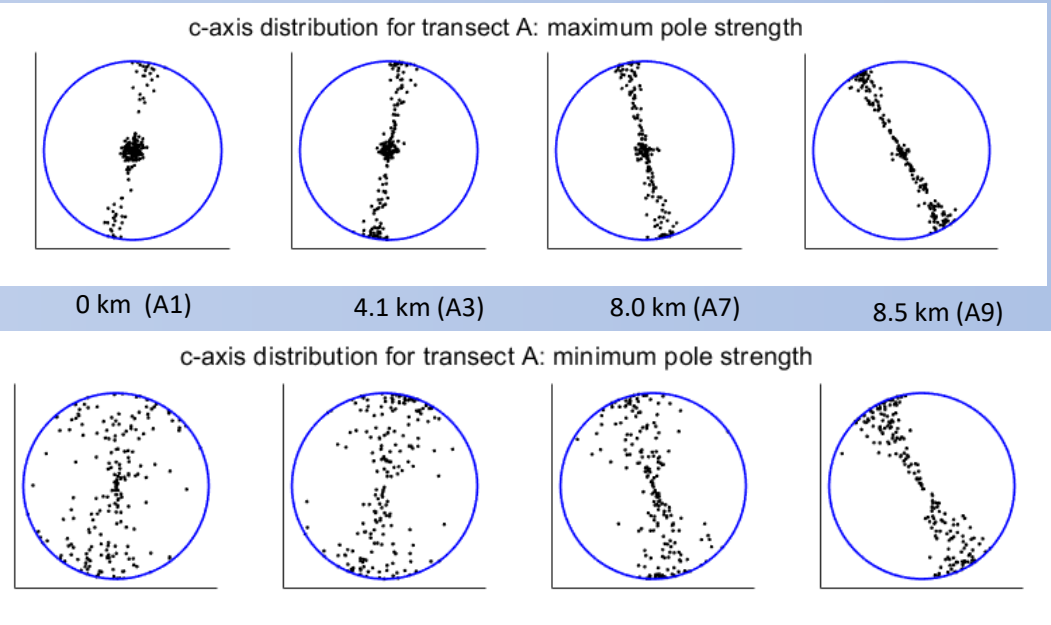

Plots consider max and min pole bounds using azimuthal equal area projection. They demonstrate combined effect of girdle rotation & strengthening.

c-axis distribution is better constrained toward shear-margin where girdle strength is higher

3.3 Spatial variation in ice fabric: Transect B

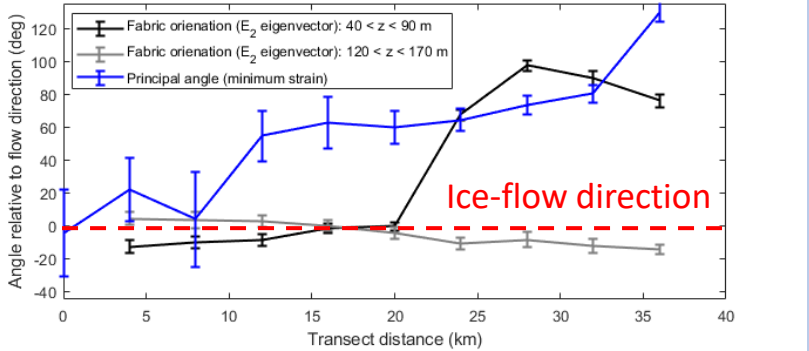

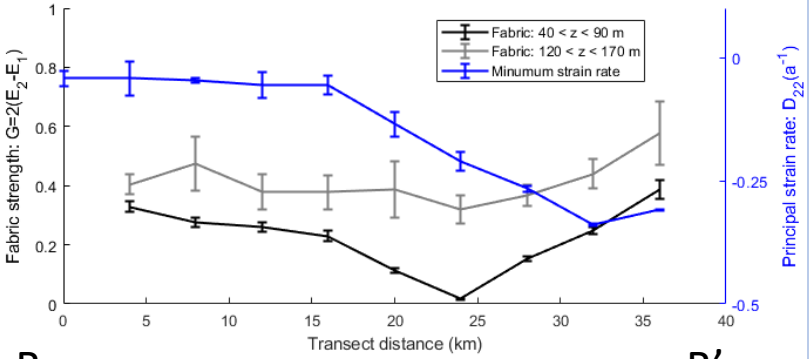

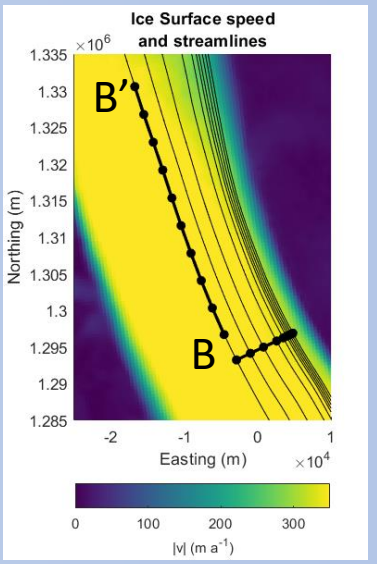

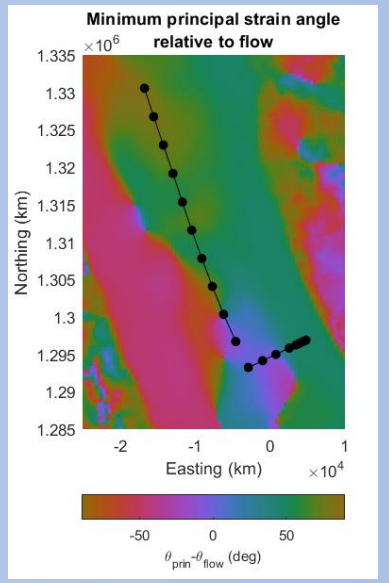

`Near-surface' fabric (40 < z < 90 m) approximately aligned with surface compression axis. Correlates with transition from along –flow compression (downstream region) to across –flow compression (upstream region).

Fabric in `deeper ice' (120 < z < 170 m) always aligned along-flow

3.4 Synthetic c-axis distributions: Transect B

Measurements at 28 & 36 km show 90-degree azimuthal rotation within the ice column!

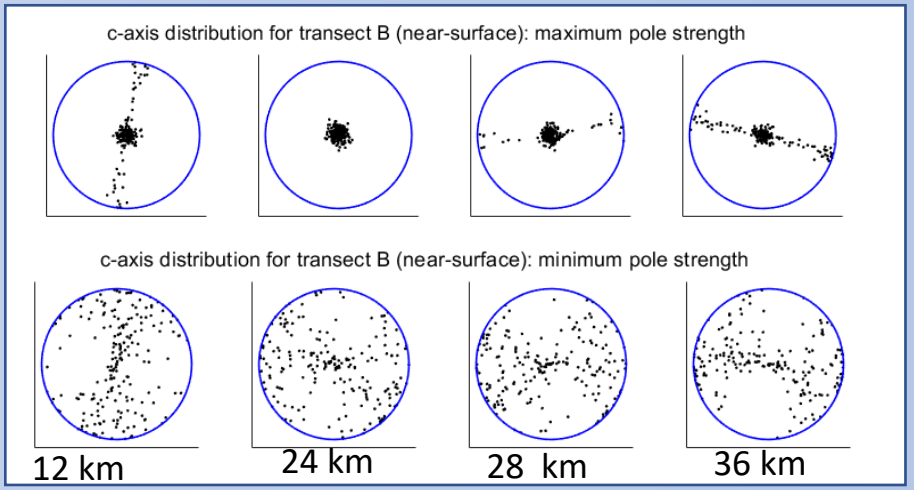

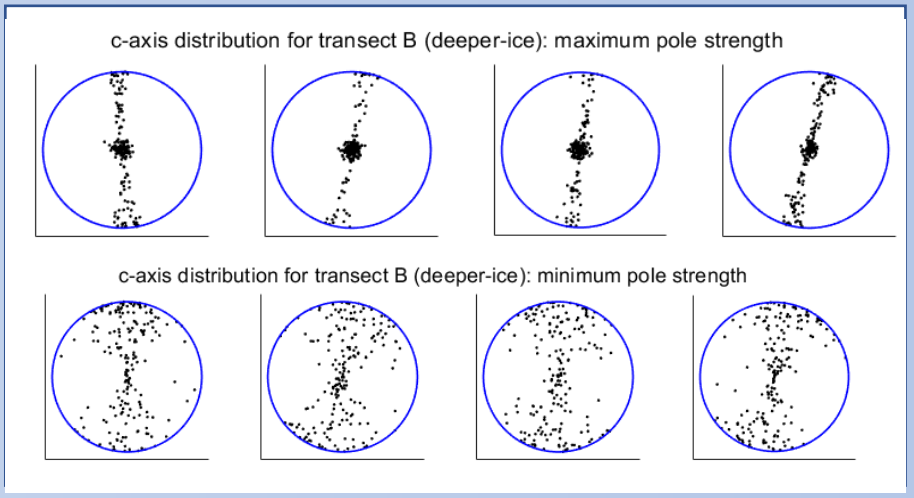

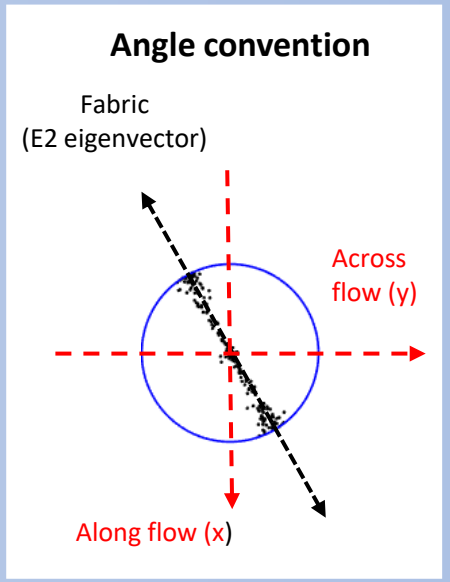

4.1 Anisotropy in ice rheology due to fabric

Transect A: near-surface layer **Transect B: near-surface layer** **Transect B: deeper ice**

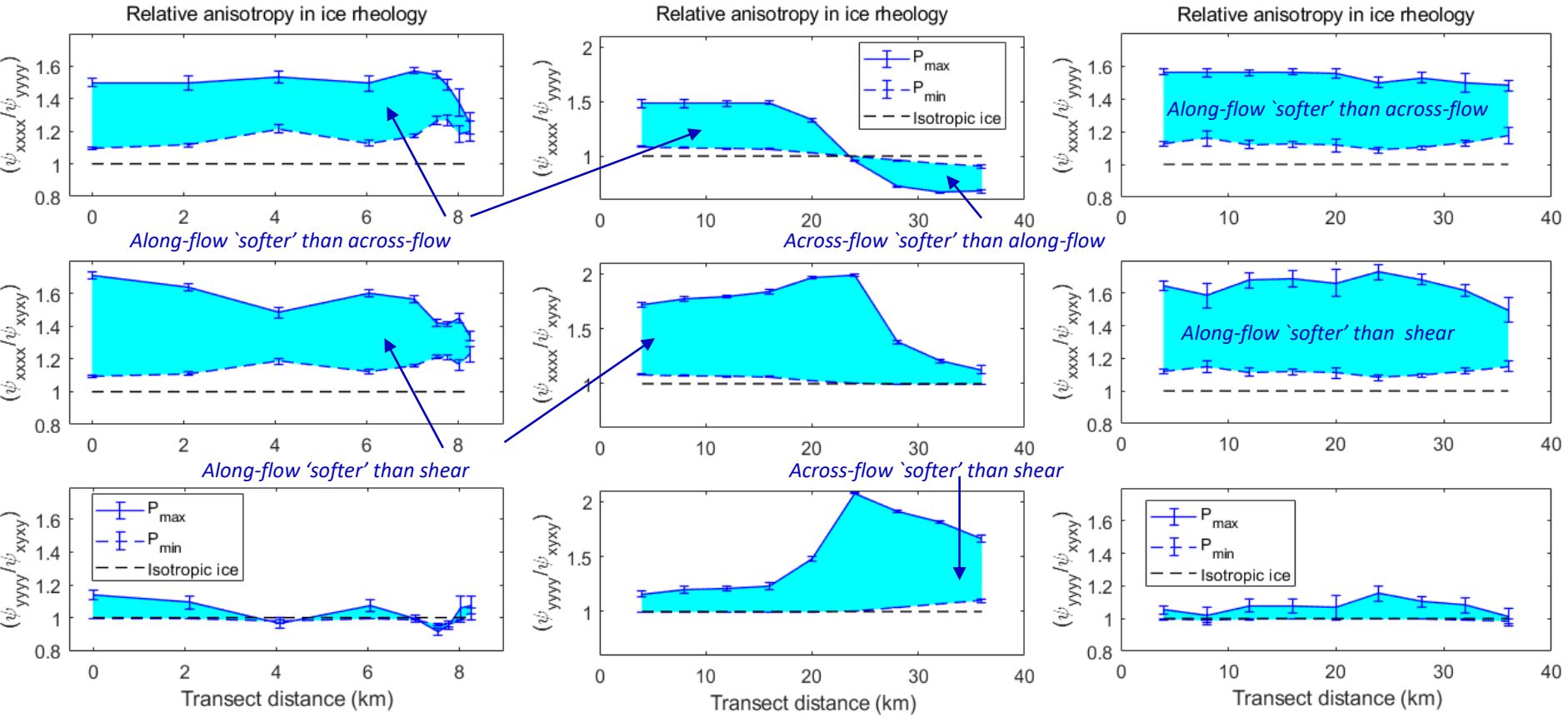

4.2 Comparison of near-surface rheology and ice surface deformation

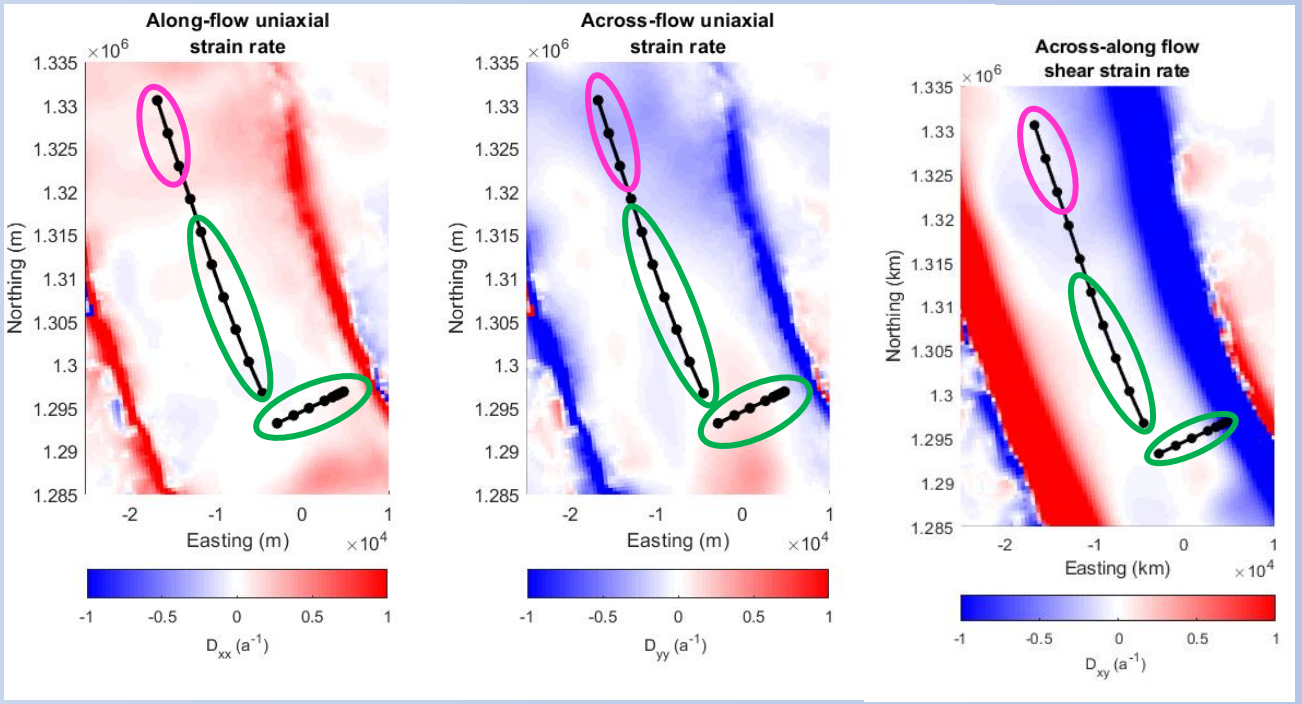

Purple region (upstream section of transect B)

- Fluidity is greater across-flow than along-flow ($\psi_{yyyy} > \psi_{xxxx}$)
- Fluidity is greater across -flow than shear ($\psi_{yyyy} > \psi_{xyxy}$)

Green regions (transect A and downstream section of transect B)

- Fluidity is greater along flow than across-flow ($\psi_{xxxx} > \psi_{yyyy}$)
- Fluidity is greater along flow than shear ($\psi_{xxxx} > \psi_{xyxy}$)

*Note: summary for green regions holds for purple regions in deeper ice z>120 m.

Summary (i) : radar fabric measurements

- Radar measurements indicate that vertical girdle fabrics with variable azimuthal orientation and strength are present in shallower ice within Rutford ice stream.

- Nearer to the ice surface (~ 40 < z < 100 m) the girdle plane has overall tendency to align with the surface compression axis. In deeper ice (~ 100 < z < 200 m) the girdle plane can be both well-aligned with the near-surface fabric or can be azimuthally rotated (extreme case ~ 90 degrees).

- In the near-surface girdle strength generally increases with compressive strain magnitude; notably toward the shear-margin.

Summary (ii) : fabric influence on rheology

- Rheological modelling reveals that the girdle fabrics result in spatially-variable horizontal anisotropy in ice rheology within the Rutford ice stream.

- Girdle ice is softer to uniaxial deformation in the direction of the girdle plane, which can result in relative enhancement of along-flow to across-flow deformation (and vice-versa). Due to girdle alignment with the compression axis, this could act as a positive dynamic feedback when ice is undergoing compression.

- When there is azimuthal fabric rotation in the ice column, different ice depths have uniaxial deformation enhanced in different directions (e.g. across-flow in the near-surface and along-flow in deeper ice). In this scenario, the surface deformation regime could substantially differ from underlying ice.

- Girdle ice is generally softer to uniaxial deformation than horizontal shear, particularly in the direction of the girdle plane. Consequently, changes in girdle strength near to the shear-margin do **not** enhance horizontal shear relative to uniaxial deformation.

Key References

J. Dall, “Ice sheet anisotropy measured with polarimetric ice sounding radar,” 30th International Geoscience and Remote Sensing Symposium, 2009.

S. Fujita, H. Maeno, and K. Matsuoka, “Radio-wave depolarization and scattering within ice sheets: a matrix-based model to link radar and ice-core measurements and its application,” Journal of Glaciology, vol. 52, no. 178, pp. 407–424, 2006.

Jordan TM, Schroeder DM, Castelletti D, Li J and Dall J (2019) A polarimetric coherence method to determine ice crystal orientation fabric from radar sounding: application to the NEEM ice core region. IEEE Transactions on Geoscience and Remote Sensing. doi: 10.1109/TGRS. 2019.2921980.

Minchew et al. 2017 Minchew, B. M., M. Simons, B. Riel, and P. Milillo (2017), Tidally induced variations in vertical and horizontal motion on Rutford Ice Stream, West Antarctica, inferred from remotely sensed observations, J. Geophys. Res. Earth Surf., 122 167–190, doi:10.1002/2016JF003971.

Martin et al. 2009 C. Martín, G. H. Gudmundsson, H. D. Pritchard, and O. Gagliardini,
“On the effects of anisotropic rheology on ice flow, internal structure, and the age-depth relationship at ice divides,” J. Geophys. Res., Earth Surf., vol. 114, no. F4, pp. 1–18, 2009.

Montagnat et al. 2014. M. Montagnat et al., “Fabric along the NEEM ice core, Greenland, and its comparison with GRIP and NGRIP ice cores,” Cryosphere, vol. 8, no. 4, pp. 1129–1138, 2014.

Nicholls KW et al. Instruments and methods a ground-based radar for measuring vertical strain rates and time-varying basal melt rates in ice sheets and shelves. Journal of Glaciology 61(230), 1079–1087. doi: 10. 3189/2015JoG15J073.

S. Fujita, H. Maeno, and K. Matsuoka, “Radio-wave depolarization and scattering within ice sheets: a matrix-based model to link radar and ice-core measurements and its application,” Journal of Glaciology, vol. 52, no. 178, pp. 407–424, 2006.